trans-Chromophore−Quencher Complexes Based on Ruthenium(II)

Benjamin J. Coe, Duane A. Friesen, David W. Thompson, and Thomas J. Meyer*

Department of Chemistry, The University of North Carolina, Chapel Hill, North Carolina 27599-3290

Received December 6, 1995[⊗]

A series of chromophore−quencher complexes, *trans*-$[Ru(bpy)_2(py^a)(py^b)]^{n+}$ (bpy = 2,2′-bipyridyl; py^a, py^b = substituted pyridyl ligands; $n = 2-4$) have been prepared and characterized. These contain combinations of the electron donor PTZ in py-PTZ (py-PTZ = 10-(4-picolyl)phenothiazine) and the electron acceptors MQ^+ (1-methyl-4,4′-bipyridinium cation), py-AQ (4-((((9,10-anthraquinon-2-yl)carbonyl)amino)methyl)pyridine), and py-MPAA (*N*-(4-pyridyl)-*β*-(1-methylpyridinium-3-yl)acrylamide cation), and 4-ethylpyridine (4-Etpy). The asymmetrical complexes ($py^a \neq py^b$) are synthesized by using the precursor *trans*-$[Ru(bpy)_2(DMSO)_2](CF_3SO_3)_2 \cdot 0.5H_2O$, which is converted into *trans*-$[Ru(bpy)_2(py\text{-}PTZ)(DMSO)](CF_3SO_3)_2 \cdot 0.5H_2O$ (**1**) by reaction with py-PTZ in DMSO/acetone at room temperature. **1** is treated with LiCl in aqueous DMF at 105 °C to prepare *trans*-$[RuCl(bpy)_2(py\text{-}PTZ)]CF_3SO_3 \cdot H_2O$ (**2**). **2** is converted into the derivatives *trans*-$[Ru(bpy)_2(py\text{-}PTZ)(4\text{-}Etpy)](PF_6)_2 \cdot 0.5H_2O$ (**5**), *trans*-$[Ru(bpy)_2(py\text{-}PTZ)(MQ^+)](PF_6)_3$ (**7**), *trans*-$[Ru(bpy)_2(py\text{-}PTZ)(py\text{-}AQ)](PF_6)_2 \cdot H_2O$ (**9**), and *trans*-$[Ru(bpy)_2(py\text{-}PTZ)(py\text{-}MPAA)](PF_6)_3 \cdot H_2O$ (**11**) by chloride abstraction at room temperature in the presence of 4-Etpy, [MQ](PF_6), py-AQ, and [py-MPAA](PF_6), respectively. The salts *trans*-$[Ru(bpy)_2(4\text{-}Etpy)(MQ^+)](PF_6)_3 \cdot H_2O$ (**6**), *trans*-$[Ru(bpy)_2(4\text{-}Etpy)(py\text{-}AQ)](PF_6)_2$ (**8**), and *trans*-$[Ru(bpy)_2(4\text{-}Etpy)(py\text{-}MPAA)](PF_6)_3$ (**10**) are synthesized by chloride abstraction from *trans*-$[RuCl(bpy)_2(4\text{-}Etpy)]PF_6 \cdot H_2O$ in the presence of [MQ](PF_6), py-AQ, or [py-MPAA](PF_6). The symmetrical complexes *trans*-$[Ru(bpy)_2(MQ^+)_2](PF_6)_4 \cdot 3H_2O$ (**3**) and *trans*-$[Ru(bpy)_2(py\text{-}PTZ)_2](PF_6)_2 \cdot H_2O$ (**4**) are synthesized by reaction of *trans*-$[Ru(bpy)_2(H_2O)_2](CF_3SO_3)_2$ with an excess of the appropriate ligand in DMF at 100 °C. Visible light irradiation of these complexes at room temperature leads to photochemical decomposition. At lower temperatures (<200 K), emission typical of $Ru^{III}-bpy^{\bullet -}$ (and $Ru^{III}-MQ^{\bullet}$) MLCT states is observed. The appearance of a thermally activated decay pathway above 150 K signals the presence of a crossing to a photochemically reactive ligand-field state. As a result, significant formation of redox-separated states by electron transfer is not observed for the redox triads *trans*-$[Ru(bpy)_2(py\text{-}PTZ)(X)]^{n+}$ (X = py-AQ, $n = 2$; X = py-MPAA or MQ^+, $n = 3$). Nonetheless, the results obtained have important implications for the stereochemical design of Ru(II)-based chromophore−quencher complexes.

Introduction

Polypyridyl complexes of Re^I, Ru^{II}, and Os^{II} have been the subject of many reports concerning photoinduced electron transfer in chromophore−quencher molecular assemblies.[1−10] Studies involving both dyad (two-component) and triad (three-component) systems have yielded valuable information concerning the fundamental aspects of electron- and energy-transfer processes. This type of excited-state behavior arises following near-UV and visible MLCT excitation of M−bpy (bpy = 2,2′-bipyridyl), M−phen (phen = 1,10-phenanthroline), or M−tpy (tpy = 2,2′:6′,2″-terpyridyl) (M = Re^I, Ru^{II}, or Os^{II}) chromophores chemically linked to electron donor (*e.g.* phenothiazine, PTZ) and/or acceptor (*e.g.* diquat, DQ^{2+}) groups capable of quenching the excited chromophore. In such systems photoinduced electron transfer can lead to the efficient formation of redox-separated states in which the oxidative and reductive equivalents occupy spatially separated sites.

Except for some Ru^{II} and Os^{II} bis-tpy complexes,[7,10] these metal complex assemblies invariably feature a *cis* relationship between the donor and acceptor sites. Hence, the separation between the photochemically produced redox equivalents is

[⊗] Abstract published in *Advance ACS Abstracts,* June 15, 1996.

(1) Balzani, V.; Scandola, F. *Supramolecular Photochemistry*; Ellis Horwood: Chichester, U.K., 1991; pp 123−151 and references therein.
(2) (a) Danielson, E.; Elliott, C. M.; Merkert, J. W.; Meyer, T. J. *J. Am. Chem. Soc.* **1987**, *109*, 2519. (b) Cooley, L. F.; Larson, S. L.; Elliott, C. M.; Kelley, D. F. *J. Phys. Chem.* **1991**, *95*, 10694. (c) Larson, S. L.; Cooley, L. F.; Elliott, C. M.; Kelley, D. F. *J. Am. Chem. Soc.* **1992**, *114*, 9504. (d) Larson, S. L.; Elliott, C. M.; Kelley, D. F. *J. Phys. Chem.* **1995**, *99*, 6530.
(3) (a) Duesing, R.; Tapolsky, G.; Meyer, T. J. *J. Am. Chem. Soc.* **1990**, *112*, 5378. (b) Chen, P.; Duesing, R.; Graff, D.; Meyer, T. J. *J. Phys. Chem.* **1991**, *95*, 5850. (c) Schoonover, J. R.; Strouse, G. F.; Chen, P.; Bates, W. D.; Meyer, T. J. *Inorg. Chem.* **1993**, *32*, 2618. (d) Strouse, G. F.; Schoonover, J. R.; Duesing, R.; Meyer, T. J. *Inorg. Chem.* **1995**, *34*, 2725.
(4) (a) Perkins, T. A.; Hauser, B. T.; Eyler, J. R.; Schanze, K. S. *J. Phys. Chem.* **1990**, *94*, 8745. (b) MacQueen, D. B.; Schanze, K. S. *J. Am. Chem. Soc.* **1991**, *113*, 7470.
(5) (a) Elliott, C. M.; Freitag, R. A.; Blaney, D. D. *J. Am. Chem. Soc.* **1985**, *107*, 4647. (b) Ryu, C. K.; Wang, R.; Schmehl, R. H.; Ferrere, S.; Ludwikow, M.; Merkert, J. W.; Headford, C. E. L.; Elliott, C. M. *J. Am. Chem. Soc.* **1992**, *114*, 430. (c) Yonemoto, E. H.; Saupe, G. B.; Schmehl, R. H.; Hubig, S. M.; Riley, R. L.; Iverson, B. L.; Mallouk, T. E. *J. Am. Chem. Soc.* **1994**, *116*, 4786. (d) Yonemoto, E. H.; Kim, Y. I.; Schmehl, R. H.; Wallin, J. D.; Shoulders, B. A.; Richardson, B. R.; Haw, J. F.; Mallouk, T. E. *J. Am. Chem. Soc.* **1994**, *116*, 10557.
(6) (a) Mecklenburg, S. L.; Peek, B. M.; Erickson, B. W.; Meyer, T. J. *J. Am. Chem. Soc.* **1991**, *113*, 8540. (b) Mecklenburg, S. L.; Peek, B. M.; Schoonover, J. R.; McCafferty, D. G.; Wall, C. G.; Erickson, B. W.; Meyer, T. J. *J. Am. Chem. Soc.* **1993**, *115*, 5479. (c) Mecklenburg, S. L.; McCafferty, D. G.; Schoonover, J. R.; Peek, B. M.; Erickson, B. W.; Meyer, T. J. *Inorg. Chem.* **1994**, *33*, 2974.
(7) (a) Collin, J.-P.; Guillerez, S.; Sauvage, J.-P.; Barigelletti, F.; De Cola, L.; Flamigni, L.; Balzani, V. *Inorg. Chem.* **1991**, *30*, 4230. (b) Collin, J.-P.; Guillerez, S.; Sauvage, J.-P.; Barigelletti, F.; De Cola, L.; Flamigni, L.; Balzani, V. *Inorg. Chem.* **1992**, *31*, 4112. (c) Sauvage, J.-P.; Collin, J.-P.; Chambron, J.-C.; Guillerez, S.; Coudret, C.; Balzani, V.; Barigelletti, F.; De Cola, L.; Flamigni, L. *Chem. Rev.* **1994**, *94*, 993.
(8) Kalyanasundaram, K.; Grätzel, M.; Nazeeruddin, M. K. *J. Phys. Chem.* **1992**, *96*, 5865.
(9) Jones, W. E., Jr.; Bignozzi, C. A.; Chen, P.; Meyer, T. J. *Inorg. Chem.* **1993**, *32*, 1167.
(10) (a) Harriman, A.; Odobel, F.; Sauvage, J.-P. *J. Am. Chem. Soc.* **1994**, *116*, 5481. (b) Collin, J.-P.; Harriman, A.; Heitz, V.; Odobel, F.; Sauvage, J.-P. *J. Am. Chem. Soc.* **1994**, *116*, 5679. (c) Odobel, F.; Sauvage, J.-P. *New J. Chem.* **1994**, *18*, 1139.

S0020-1669(95)01546-1 CCC: $12.00

Chart 1

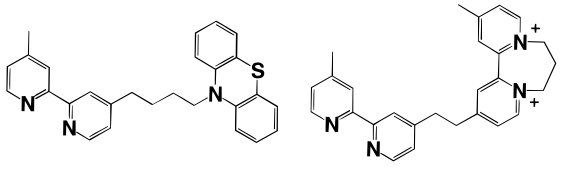

Mebpy-PTZ Mebpy-3DQ^{2+}

relatively short and through-space back electron transfer potentially rapid. This may be a major cause of the relatively short redox-separated-state lifetime observed in the first metal-based chromophore−quencher triad [Ru(Mebpy-3DQ^{2+})(Mebpy-PTZ)$_2$]$^{4+}$ (Mebpy-3DQ^{2+} and Mebpy-PTZ are shown in Chart 1), where $\tau_{sep} \approx 165$ ns at room temperature in dichloromethane.[2] Because of the methylene links between the metal−polypyridyl unit and the quencher sites, through-bond electronic coupling is small. Following MLCT excitation and electron transfer in [Re(CO)$_3$(bpy-PTZ)(MQ$^+$)]$^{2+}$ (bpy-PTZ = 4-methyl-4′-(phenothiazine-10-ylmethyl)-2,2′-bipyridine, MQ$^+$ = 1-methyl-4,4′-bipyridinium cation), the distance of closest approach (center-to-center) between the redox pair −PTZ$^{\bullet+}$/MQ$^\bullet$ is only ∼5 Å and τ = 15 ns for the redox-separated state in dichloroethane at room temperature.[3d,11]

We are interested in exploring the *trans* geometry in chromophore−quencher complexes as a way of increasing redox pair separation distances and increasing the lifetimes of redox-separated states. We have been investigating routes for the preparation of functionalized *trans* complexes and have developed a stepwise synthetic strategy by which 4-substituted pyridyl ligands are attached to the *trans*-{Ru(bpy)$_2$}$^{2+}$ core by using *trans*-[Ru(bpy)$_2$(DMSO)$_2$](CF$_3$SO$_3$)$_2$ as a precursor.[12] We report here the application of this procedure to the preparation of chromophore−quencher complexes and the photophysical properties of the resulting complexes.

Experimental Section

Materials and Procedures. The salts *trans*-[Ru(bpy)$_2$(H$_2$O)$_2$](CF$_3$SO$_3$)$_2$,[13] *trans*-[Ru(bpy)$_2$(DMSO)$_2$](CF$_3$SO$_3$)$_2$·0.5H$_2$O,[12] and *trans*-[RuCl(bpy)$_2$(4-Etpy)]PF$_6$·H$_2$O[12] were prepared according to previously published procedures. The ligands 10-(4-picolyl)phenothiazine (py-PTZ)[14] and 1-methyl-4,4′-bipyridinium iodide ([MQ]I)[15] were synthesized by established methods. The salt [MQ]PF$_6$ was prepared by metathesis with NH$_4$PF$_6$. The ligand salt *N*-(4-pyridyl)-*β*-(1-methylpyridinium-3-yl)acrylamide hexafluorophosphate ([py-MPAA]PF$_6$) was available from a previous study.[16] All other reagents were obtained commercially and used as supplied. All reactions were carried out in the dark under an atmosphere of argon. Products were dried at room temperature in a vacuum desiccator for *ca.* 15 h prior to characterization. For measurements in 2-methyltetrahydrofuran (where the PF$_6^-$ salts were insoluble), the complexes were converted to the tetrakis(3,5-bis(trifluoromethyl)phenyl)borate (BAr$_4^-$) salts by metathesis with Na(BAr$_4$) in dichloromethane.[17]

In the following descriptions, numbers are used to represent the *trans*-Ru(II) complex cations, whereas the salts are labeled by a number followed by the counteranion (e.g. **4-PF$_6$**).

Synthesis of 4-((((9,10-Anthraquinon-2-yl)carbonyl)amino)methyl)pyridine (py-AQ). A solution of 9,10-anthraquinone-2-carboxylic acid (2.01 g, 7.96 mmol), pyBOP (6.22 g, 11.95 mmol), 1-hydroxybenzotriazole (2.45 g, 16.0 mmol), and 4-methylmorpholine (1.8 mL, 16.4 mmol) in DMF (60 mL) was stirred at room temperature for 2 min. 4-(Amino-methyl)pyridine (1 mL) was added, the solution stirred for 1 min, and 4-(dimethylamino)pyridine (0.97 g, 7.94 mmol) added. The reaction mixture was stirred at room temperature for 4 h to give a turbid brown solution. Water (250 mL) was added and the precipitate collected by filtration, washed with 0.5 M aqueous NaHCO$_3$ solution, washed with water, and dried. The product was dissolved through the frit in DMF to leave behind some gray solid and precipitated by the addition of water. The solid was collected by filtration, washed with water, and dried to yield a cream-colored powder: yield 2.16 g, 75%; δ_H (CD$_3$SOCD$_3$) 9.64 (1 H, t, J = 5.8 Hz, *NH*), 8.73 (1 H, d, J = 1.5 Hz, *1*), 8.53 (2 H, t, J = 5.9 Hz, *py*), 8.43−8.21 (4 H, c m, *AQ*), 8.02−7.93 (2 H, c m, *AQ*), 7.36 (2 H, d, J = 5.9 Hz, *py*), 4.57 (2 H, d, J = 5.9 Hz, *CH$_2$*); ν(NH) 3495 (m) cm^{-1}, ν(CO)$_{quinone}$ 1678 (s) cm^{-1}, ν(CO)$_{amide}$ 1647 (s) cm^{-1}. Anal. Calcd for C$_{21}$H$_{14}$N$_2$O$_3$·0.9H$_2$O: C, 70.34; H, 4.44; N, 7.81. Found: C, 70.43; H, 4.37; N, 7.80.

Synthesis of *trans*-[Ru(bpy)$_2$(py-PTZ)(DMSO)](CF$_3$SO$_3$)$_2$·0.5H$_2$O (1-CF$_3$SO$_3$). A solution of *trans*-[Ru(bpy)$_2$(DMSO)$_2$](CF$_3$SO$_3$)$_2$·0.5H$_2$O (400 mg, 0.456 mmol) and py-PTZ (600 mg, 2.07 mmol) in 40% DMSO/acetone (10 mL) was stirred at room temperature for 5 days. After this time acetone lost due to evaporation was replaced by the addition of further acetone (5 mL) and the solution was stirred for another 9 days. The addition of diethyl ether (200 mL) afforded a yellow precipitate, which was collected by filtration, washed with diethyl ether, and dried: yield 494 mg, 99%; δ_H (CD$_3$SOCD$_3$) 9.62 (4 H, d, J = 5.5 Hz, *bpy* × 2), 8.58 (4 H, d, J = 7.6 Hz, *bpy* × 2), 8.30 (4 H, t, J = 7.7 Hz, *bpy* × 2), 7.93 (4 H, t, J = 6.3 Hz, *bpy* × 2), 7.72 (2 H, d, J = 6.4 Hz, *py*-CH$_2$PTZ), 7.14 (2 H, dd, J = 7.3, 1.7 Hz, pyCH$_2$-*PTZ*), 7.07−6.89 (6 H, c m, *py*-CH$_2$-*PTZ*), 6.51 (2 H, d, J = 7.4 Hz, pyCH$_2$-*PTZ*), 5.05 (2 H, s, py-*CH$_2$*-PTZ), 2.57 (6 H, s, *Me$_2$*SO). Anal. Calcd for C$_{42}$H$_{36}$F$_6$N$_6$O$_7$RuS$_4$·0.5H$_2$O: C, 46.32; H, 3.42; N, 7.72. Found: C, 46.34; H, 3.19; N, 7.87. (Note: The excess py-PTZ in the filtrate was recovered by evaporation of the diethyl ether followed by the addition of water. The solid was collected by filtration, washed with water, and dried for further use.)

Synthesis of *trans*-[RuCl(bpy)$_2$(py-PTZ)]CF$_3$SO$_3$·H$_2$O (2-CF$_3$SO$_3$). **1-CF$_3$SO$_3$** (254 mg, 0.233 mmol) was added to a saturated solution of LiCl in 1/1 (v/v) DMF/water (8 mL), and the mixture was heated at 105 °C for 2 h. The reaction mixture was cooled to room temperature, and water (40 mL) was added. The dark solid was collected by filtration and washed with water. The crude product was dissolved in DMF, precipitated by the addition of diethyl ether, collected by filtration, and washed with diethyl ether. Further purification was achieved by recrystallization from DMF/diethyl ether. In order to eliminate any solvent(s) of crystallization, the product was finally precipitated from DMF/acetone by the addition of diethyl ether. The dark purple solid was collected by filtration, washed with diethyl ether, and dried: yield 120 mg, 57%; δ_H (CD$_3$SOCD$_3$) 9.51 (4 H, d, J = 5.5 Hz, *bpy* × 2), 8.59 (4 H, d, J = 7.6 Hz, *bpy* × 2), 8.14 (4 H, t, J = 7.4 Hz, *bpy* × 2), 7.78−7.72 (6 H, c m, *bpy* × 2, *py*-CH$_2$PTZ), 7.12 (2 H, dd, J = 7.2, 1.8 Hz, pyCH$_2$-*PTZ*), 7.02−6.85 (6 H, c m, *py*-CH$_2$-*PTZ*), 6.53 (2 H, dd, J = 7.9, 1.0 Hz, pyCH$_2$-*PTZ*), 5.00 (2 H, s, py-*CH$_2$*-PTZ). Anal. Calcd for C$_{39}$H$_{30}$ClF$_3$N$_6$O$_3$RuS$_2$·H$_2$O: C, 51.68; H, 3.56; N, 9.27. Found: C, 51.79; H, 3.36; N, 9.18.

Synthesis of *trans*-[Ru(bpy)$_2$(MQ$^+$)$_2$](PF$_6$)$_4$·3H$_2$O (3-PF$_6$). A solution of *trans*-[Ru(bpy)$_2$(H$_2$O)$_2$](CF$_3$SO$_3$)$_2$ (50 mg, 0.067 mmol) and [MQ]PF$_6$ (439 mg, 1.39 mmol; 21 equiv) in DMF (1.5 mL) was heated at 100 °C for 1 h. The resulting dark orange solution was cooled to room temperature and the product precipitated by the addition of aqueous NH$_4$PF$_6$. The orange solid was collected by filtration and washed with water. The crude product was dissolved in DMF/acetone, precipitated with aqueous NH$_4$PF$_6$, collected by filtration, washed with water, and dried: yield 70 mg, 75%; δ_H (CD$_3$SOCD$_3$) 9.76 (4 H, d, J = 5.5 Hz, *bpy* × 2), 9.02 (4 H, d, J = 6.6 Hz, py-*C$_5$H$_4$N$^+$*-Me × 2), 8.70 (4 H, d, J = 8.0 Hz, *bpy* × 2), 8.36 (4 H, d, J = 6.6 Hz, py-*C$_5$H$_4$N$^+$*-Me × 2), 8.28 (4 H, t, J = 7.8 Hz, *bpy* × 2), 8.14 (4 H, d, J = 6.3 Hz, *py*-C$_5$H$_4$N$^+$-Me × 2), 7.94 (4 H, t, J = 6.4 Hz, bpy × 2), 7.60 (4 H, d, J = 6.4 Hz, *py*-C$_5$H$_4$N$^+$-Me × 2), 4.31 (6 H, s, pyC$_5$H$_4$N$^+$-

(11) Duesing, R. Ph.D. Dissertation, The University of North Carolina at Chapel Hill, 1988.
(12) Coe, B. J.; Meyer, T. J.; White, P. S. *Inorg. Chem.* **1993**, *32*, 4012.
(13) Dobson, J. C.; Meyer, T. J. *Inorg. Chem.* **1988**, *27*, 3283.
(14) Chen, P.; Westmoreland, T. D.; Danielson, E.; Schanze, K. S.; Anthon, D.; Neveux, P. E., Jr.; Meyer, T. J. *Inorg. Chem.* **1987**, *26*, 1116.
(15) Curtis, J. C.; Sullivan, B. P.; Meyer, T. J. *Inorg. Chem.* **1983**, *22*, 224.
(16) Calvert, J. M.; Schmehl, R. H.; Sullivan, B. P.; Facci, J. S.; Meyer, T. J.; Murray, R. W. *Inorg. Chem.* **1983**, *22*, 2151.
(17) Brookhart, M. *Organometallics* **1992**, *11*, 3920.

Me × 2). Anal. Calcd for $C_{42}H_{38}F_{24}N_8P_4Ru\cdot 3H_2O$: C, 36.30; H, 3.19; N, 8.06. Found: C, 36.45; H, 2.80; N, 7.96.

Synthesis of *trans*-[Ru(bpy)$_2$(py-PTZ)$_2$](PF$_6$)$_2$·H$_2$O (4-PF$_6$). A solution of *trans*-[Ru(bpy)$_2$(H$_2$O)$_2$](CF$_3$SO$_3$)$_2$ (50 mg, 0.067 mmol) and py-PTZ (409 mg, 1.41 mmol; 21 equiv) in DMF (3 mL) was heated at 100 °C for 1 h. The resulting dark orange solution was cooled to room temperature and the product precipitated by addition to diethyl ether (100 mL). The orange solid was collected by filtration and washed with diethyl ether. The crude product was dissolved in DMF/acetone, precipitated with aqueous NH_4PF_6, collected by filtration, washed with water, and dried. Further purification was effected by two recrystallizations from DMF/diethyl ether followed by precpitation from DMF/acetone by the addition of diethyl ether. The red-orange solid was collected by filtration, washed with diethyl ether, and dried: yield 61 mg, 70%; δ_H (CD_3SOCD_3) 9.58 (4 H, d, J = 5.6 Hz, *bpy* × 2), 8.58 (4 H, d, J = 8.1 Hz, *bpy* × 2), 8.17 (4 H, t, J = 7.7 Hz, *bpy* × 2), 7.80−7.75 (8 H, c m, *bpy* × 2, *py*-CH$_2$PTZ × 2), 7.13 (4 H, dd, J = 7.0, 1.7 Hz, pyCH$_2$-*PTZ* × 2), 7.02−6.87 (12 H, c m, *py*-CH$_2$-*PTZ* × 2), 6.50 (4 H, d, J = 7.3 Hz, pyCH$_2$-*PTZ* × 2), 5.03 (4 H, s, py-*CH*$_2$-PTZ × 2). Anal. Calcd for $C_{56}H_{44}F_{12}N_8P_2RuS_2\cdot H_2O$: C, 51.65; H, 3.40; N, 8.61. Found: C, 51.58; H, 3.48; N, 8.53.

Synthesis of *trans*-[Ru(bpy)$_2$(py-PTZ)(4-Etpy)](PF$_6$)$_2$·0.5H$_2$O (5-PF$_6$). A solution of **2-CF$_3$SO$_3$** (50 mg, 0.055 mmol), TlPF$_6$ (34 mg, 0.097 mmol), and 4-ethylpyridine (1 mL) in DMF (3 mL) and 50% aqueous acetone (20 mL) was stirred at room temperature for 72 h. The addition of aqueous NH_4PF_6 afforded an orange precipitate, which was collected by filtration and washed with water. The product was dissolved through the frit in DMF/acetone and precipitated by the addition of diethyl ether. The red-orange solid was collected by filtration, washed with diethyl ether, and dried: yield 60 mg, 98%; δ_H (CD_3SOCD_3) 9.63 (4 H, d, J = 5.5 Hz, *bpy* × 2), 8.61 (4 H, d, J = 7.4 Hz, *bpy* × 2), 8.20 (4 H, t, J = 7.6 Hz, *bpy* × 2), 7.85−7.78 (6 H, c m, *bpy* × 2, *py*-CH$_2$PTZ), 7.68 (2 H, d, J = 6.5 Hz, *py*-Et), 7.14 (2 H, dd, J = 7.1, 2.0 Hz, pyCH$_2$-*PTZ*), 7.03−6.89 (8 H, c m, *py*-CH$_2$-*PTZ*, *py*-Et), 6.51 (2 H, dd, J = 7.8, 1.3 Hz, pyCH$_2$-*PTZ*), 5.04 (2 H, s, py-*CH*$_2$-PTZ), 2.42 (2 H, q, J = 7.6 Hz, py-*CH*$_2$-Me), 0.94 (3 H, t, J = 7.6 Hz, pyCH$_2$-*Me*). Anal. Calcd for $C_{45}H_{39}F_{12}N_7P_2RuS\cdot 0.5H_2O$: C, 48.70; H, 3.63; N, 8.83. Found: C, 48.73; H, 3.45; N, 8.81.

Synthesis of *trans*-[Ru(bpy)$_2$(4-Etpy)(MQ$^+$)](PF$_6$)$_3$·H$_2$O (6-PF$_6$). A solution of *trans*-[RuCl(bpy)$_2$(4-Etpy)]PF$_6$·H$_2$O (50 mg 0.070 mmol), AgCF$_3$CO$_2$ (23 mg, 0.104 mmol), and [MQ]PF$_6$ (1.71 g, 5.41 mmol) in 40% aqueous acetone (14 mL) was stirred at room temperature for 7 days. The addition of water (40 mL) afforded an orange precipitate, which was collected by filtration and washed with water. The product was dissolved through the frit in DMF/acetone and precipitated by the addition of aqueous NH_4PF_6. The red-orange solid was collected by filtration, washed with water, and dried: yield 78 mg, 98%; δ_H (CD_3SOCD_3) 9.72 (4 H, d, J = 5.4 Hz, *bpy* × 2), 9.01 (2 H, d, J = 6.5 Hz, py-*C$_5$H$_4$N$^+$*-Me), 8.68 (4 H, d, J = 7.9 Hz, *bpy* × 2), 8.36 (2 H, d, J = 6.5 Hz, py-*C$_5$H$_4$N$^+$*-Me), 8.26 (4 H, t, J = 7.7 Hz, *bpy* × 2), 8.12 (2 H, d, J = 6.2 Hz, *py*-C$_5$H$_4$N$^+$-Me), 7.90 (4 H, t, J = 6.4 Hz, bpy × 2), 7.71 (2 H, d, J = 6.0 Hz, *py*-Et), 7.59 (2 H, d, J = 6.3 Hz, *py*-C$_5$H$_4$N$^+$-Me), 6.94 (2 H, d, J = 6.0 Hz, *py*-Et), 4.31 (3 H, s, pyC$_5$H$_4$N$^+$-*Me*), 2.45 (2 H, q, J = 7.5 Hz, py-*CH*$_2$-Me), 0.96 (3 H, t, J = 7.5 Hz, pyCH$_2$-*Me*). Anal. Calcd for $C_{38}H_{36}F_{18}N_7P_3Ru\cdot H_2O$: C, 39.87; H, 3.35; N, 8.57. Found: C, 40.07; H, 3.11; N, 8.49.

Synthesis of *trans*-[Ru(bpy)$_2$(py-PTZ)(MQ$^+$)](PF$_6$)$_3$ (7-PF$_6$). A solution of **2-CF$_3$SO$_3$** (50 mg, 0.055 mmol), AgCF$_3$CO$_2$ (15 mg, 0.068 mmol), and [MQ]PF$_6$ (1.36 g, 4.31 mmol) in DMF (2.5 mL) and 30% aqueous acetone (14 mL) was stirred at room temperature for 9 days. The addition of water (40 mL) afforded an orange precipitate, which was collected by filtration and washed with water. The product was dissolved through the frit in DMF/acetone and precipitated by the addition of aqueous NH_4PF_6. The red-orange solid was collected by filtration, washed with water, and dried. This yielded 67 mg of crude product, which was found to contain *ca*. 90% **7-PF$_6$** by ^{1}H NMR spectroscopy. Purification was effected by several recrystallizations from DMF/diethyl ether followed by precipitation to remove solvent(s) of crystallization: yield 46 mg, 64%; δ_H (CD_3SOCD_3) 9.67 (4 H, d, J = 5.5 Hz, *bpy* × 2), 9.00 (2 H, d, J = 6.8 Hz, py-*C$_5$H$_4$N$^+$*-Me), 8.64 (4 H, d, J = 7.6 Hz, *bpy* × 2), 8.35 (2 H, d, J = 6.8 Hz, py-*C$_5$H$_4$N$^+$*-Me), 8.23 (4 H, t, J = 7.7 Hz, *bpy* × 2), 8.12 (2 H, d, J = 6.6 Hz, *py*-C$_5$H$_4$N$^+$-Me), 7.89−7.80 (6 H, c m, *bpy* × 2, *py*-CH$_2$PTZ), 7.57 (2 H, d, J = 6.7 Hz, *py*-C$_5$H$_4$N$^+$-Me), 7.15 (2 H, dd, J = 7.1, 1.9 Hz, pyCH$_2$-*PTZ*), 7.05−6.89 (6 H, c m, *py*-CH$_2$-*PTZ*), 6.51 (2 H, dd, J = 7.8, 1.2 Hz, pyCH$_2$-*PTZ*), 5.05 (2 H, s, py-*CH*$_2$-PTZ), 4.30 (3 H, s, pyC$_5$H$_4$N$^+$-*Me*). Anal. Calcd for $C_{49}H_{41}F_{18}N_8P_3RuS$: C, 44.93; H, 3.15; N, 8.55. Found: C, 44.94; H, 3.08; N, 8.47.

Synthesis of *trans*-[Ru(bpy)$_2$(4-Etpy)(py-AQ)](PF$_6$)$_2$ (8-PF$_6$). A solution of *trans*-[RuCl(bpy)$_2$(4-Etpy)]PF$_6$·H$_2$O (35 mg, 0.049 mmol), AgPF$_6$ (17 mg, 0.067 mmol), and py-AQ·0.9H$_2$O (0.67 g, 1.87 mmol) in 15% aqueous DMF (12 mL) was stirred at room temperature for 14 days. The addition of aqueous NH_4PF_6 afforded a large amount of red-orange precipitate which was collected by filtration, washed with water, and dried. The excess ligand was removed by washing with $CHCl_3$ (*ca*. 100 mL) until only a small amount of red-orange solid remained in the frit. The product was dissolved through the frit in DMF/acetone and precipitated by the addition of $CHCl_3$. The solid was collected by filtration and washed with $CHCl_3$ and the reprecipitation procedure repeated a total of three times to yield the pure product as a red-orange solid: yield 35 mg, 63%; δ_H (CD_3SOCD_3) 9.68 (4 H, d, J = 5.5 Hz, *bpy* × 2), 9.44 (1 H, t, J = 5.5 Hz, *NH*), 8.65 (4 H, d, J = 7.8 Hz, *bpy* × 2), 8.59 (1 H, s, *1*), 8.32−8.18 (8 H, c m, *bpy* × 2, *AQ*), 8.01−7.78 (8 H, c m, *bpy* × 2, *py-AQ*), 7.69 (2 H, d, J = 6.4 Hz, *py*-Et), 6.99 (2 H, d, J = 6.4 Hz, *py*-AQ), 6.92 (2 H, d, J = 6.5 Hz, *py*-Et), 4.39 (2 H, d, J = 5.2 Hz, *CH*$_2$-NH), 2.43 (2 H, q, J = 7.6 Hz, py-*CH*$_2$-Me), 0.95 (3 H, t, J = 7.6 Hz, pyCH$_2$-*Me*); ν(CO)$_{quinone}$ 1676 (s) cm^{-1}, ν(CO)$_{amide}$ 1660 sh (s) cm^{-1}. Anal. Calcd for $C_{48}H_{39}F_{12}N_7O_3P_2Ru$: C, 50.01; H, 3.41; N, 8.50. Found: C, 50.54; H, 3.34; N, 8.46.

Synthesis of *trans*-[Ru(bpy)$_2$(py-PTZ)(py-AQ)](PF$_6$)$_2$·H$_2$O (9-PF$_6$). A solution of *trans*-[RuCl(bpy)$_2$(py-PTZ)]CF$_3$SO$_3$·H$_2$O (53 mg, 0.058 mmol), AgPF$_6$ (20 mg, 0.079 mmol), and py-AQ·0.9H$_2$O (1.44 g, 4.02 mmol) in 8% aqueous DMF (35 mL) was stirred at room temperature for 14 days. The crude product was isolated as for **8-PF$_6$** and purified by several recrystallizations from DMF/diethyl ether to give a red-orange solid: yield 45 mg, 57%; δ_H (CD_3SOCD_3) 9.62 (4 H, d, J = 5.6 Hz, *bpy* × 2), 9.44 (1 H, t, J = 5.6 Hz, *NH*), 8.63, 8.59 (5 H, s s, *bpy* × 2, *1*), 8.26−8.15 (8 H, c m, *bpy* × 2, *py-AQ*), 8.01−7.93 (2 H, c m, py-*AQ*), 7.85−7.78 (8 H, c m, *bpy* × 2, *py*-PTZ, py-*AQ*), 7.13 (2 H, dd, J = 7.1, 2.0 Hz, *PTZ*), 7.03−6.87 (8 H, c m, *py-PTZ*, *py*-AQ), 6.50 (2 H, dd, J = 7.8, 1.2 Hz, *PTZ*), 5.03 (2 H, s, py-*CH*$_2$-PTZ), 4.38 (2 H, d, J = 5.3 Hz, *CH*$_2$-NH); ν(CO)$_{quinone}$ 1676 (s) cm^{-1}, ν(CO)$_{amide}$ 1660 sh (s) cm^{-1}. Anal. Calcd for $C_{59}H_{44}F_{12}N_8O_3P_2RuS\cdot H_2O$: C, 52.33; H, 3.42; N, 8.27. Found: C, 52.55; H, 3.56; N, 8.20.

Synthesis of *trans*-[Ru(bpy)$_2$(4-Etpy)(py-MPAA)](PF$_6$)$_3$ (10-PF$_6$). A solution of *trans*-[RuCl(bpy)$_2$(4-Etpy)]PF$_6$·H$_2$O (35 mg, 0.049 mmol), AgCF$_3$CO$_2$ (16 mg, 0.072 mmol), and [py-MPAA]PF$_6$ (1.53 g, 3.97 mmol) in 40% aqueous DMF (10 mL) was stirred at room temperature for 7 days. The addition of aqueous NH_4PF_6 afforded an orange precipitate, which was collected by filtration and washed with water. The product was dissolved through the frit in DMF/acetone, precipitated by the addition of water, collected by filtration, and washed with water. This reprecipitation procedure was repeated twice more and the red-orange product dried: yield 52 mg, 90%; δ_H (CD_3SOCD_3) 10.94 (1 H, s, *NH*), 9.68 (4 H, d, J = 5.6 Hz, *bpy* × 2), 9.24 (1 H, s, *a*), 8.95 (1 H, d, J = 6.0 Hz, *d* or *b*), 8.73−8.64 (5 H, c m, *bpy* × 2, *d* or *b*), 8.23 (4 H, t, J = 7.7 Hz, *bpy* × 2), 8.19−8.12 (1 H, c m, *c*), 7.87 (4 H, t, J = 6.4 Hz, *bpy* × 2), 7.73−7.63 (5 H, c m, *py*-MPAA, *py*-Et, C*H*═), 7.31 (2 H, d, J = 6.9 Hz, *py*-MPAA), 6.94−6.86 (3 H, c m, *py*-Et, ═C*H*), 4.33 (3 H, s, py-*Me*), 2.44 (2 H, q, J = 7.6 Hz, py-*CH*$_2$-Me), 0.96 (3 H, t, J = 7.6 Hz, pyCH$_2$-*Me*); ν(CO) 1697 (m) cm^{-1}. Anal. Calcd for $C_{41}H_{39}F_{18}N_8OP_3Ru$: C, 41.18; H, 3.29; N, 9.37. Found: C, 41.29; H, 3.44; N, 9.23.

Synthesis of *trans*-[Ru(bpy)$_2$(py-PTZ)(py-MPAA)](PF$_6$)$_3$·H$_2$O (11-PF$_6$). A solution of *trans*-[RuCl(bpy)$_2$(py-PTZ)]CF$_3$SO$_3$·H$_2$O (50 mg, 0.055 mmol), AgCF$_3$CO$_2$ (15 mg, 0.068 mmol), and [py-MPAA]PF$_6$ (1.72 g, 4.46 mmol) in 30% aqueous DMF (10 mL) was stirred at room temperature for 10 days. The crude product was isolated as for **10-PF$_6$** and purified by several recrystallizations from DMF/diethyl ether, followed by precipitation to eliminate DMF of crystallization to yield a red-orange solid: yield 70 mg, 91%; δ_H (CD_3SOCD_3) 10.94 (1 H, s, *NH*), 9.62 (4 H, d, J = 5.6 Hz, *bpy* × 2), 9.23 (1 H, s, *a*), 8.95 (1 H,

d, $J = 5.9$ Hz, *d* or *b*), 8.70 (1 H, d, $J = 8.1$ Hz, *d* or *b*), 8.62 (4 H, d, $J = 8.1$ Hz, *bpy* × 2), 8.24−8.11 (5 H, c m, *bpy* × 2, *c*), 7.86−7.62 (9 H, c m, *bpy* × 2, C*H*═, *py*-PTZ, *py*-MPAA), 7.30 (2 H, d, $J = 6.5$ Hz, *py*-MPAA), 7.14 (2 H, d, $J = 6.3$ Hz, *PTZ*), 7.03−6.85 (7 H, c m, *py-PTZ*, ═C*H*), 6.51 (2 H, d, $J = 7.6$ Hz, *PTZ*), 5.04 (2 H, s, py-CH_2-PTZ), 4.32 (3 H, s, py-*Me*); ν(CO) 1701 (m) cm^{-1}. Anal. Calcd for $C_{52}H_{44}F_{18}N_9OP_3RuS \cdot H_2O$: C, 44.71; H, 3.32; N, 9.02. Found: C, 44.61; H, 3.41; N, 9.02.

Physical Measurements. ^{1}H NMR spectra were recorded on a Bruker AC200 spectrometer, and all shifts are referenced to TMS. Proton labels are shown in Figure 1. IR spectra were obtained as KBr disks with a Mattson Galaxy Series FTIR 5000 instrument. UV−visible spectra were recorded on a Hewlett-Packard 8451A diode array spectrophotometer. Elemental analyses were performed by ORS, Whitesboro, NY. Cyclic voltammetric measurements were carried out by using a PAR Model 173 potentiostat with a PAR Model 175 universal programmer. A three-compartment cell was used with an SCE reference electrode separated from a Pt-disk working electrode (surface area 0.031 cm^2) and Pt-wire auxiliary electrode by a medium-porosity glass frit. Spectrophotometric grade acetonitrile (Burdick and Jackson) was used as received, and tetra-*n*-butylammonium hexafluorophosphate, $[N(n\text{-}C_4H_9)_4]PF_6$, doubly recrystallized from ethanol and dried in vacuo, was used as supporting electrolyte. Solutions containing 10^{-3} M analyte (0.1 M electrolyte) were deaerated for 5 min by a vigorous Ar purge. All $E_{1/2}$ values were calculated from $(E_{pa} + E_{pc})/2$ at a scan rate of 200 mV s^{-1} with no correction for junction potentials.

Steady-state emission spectra were obtained on a Spex F212 photon-counting spectrofluorometer with a cooled Hamamatsu R666-10 PMT. Spectra were routinely corrected for instrument response. Emission quantum yields, ϕ_{em}, were measured in optically dilute (absorbance <0.25) 4/5 v/v propionitrile/butyronitrile solutions at 77 K (in a quartz finger Dewar) relative to $[Ru(bpy)_3](PF_6)_2$, where $\phi_{em} = 0.38$ (4:1 ethanol/methanol v/v).[18a] The emission quantum yields were calculated by using eq 1.[18b] *A* is the absorbance of the sample at the excitation

$$\phi_{em}{}^{u} = \phi_{em}{}^{std}\left(\frac{A^{std}}{A^{u}}\right)\left(\frac{I^{u}}{I^{std}}\right)\left(\frac{n_D{}^{u}}{n_D{}^{std}}\right)^2 \qquad (1)$$

wavelength, *I* is the integrated intensity of the emission band, n_D is the refractive index of the solvent, and the superscripts u and std refer to the unknown and standard, respectively. In these measurements it was assumed that $n_D{}^u/n_D{}^{std}$ does not change significantly between 298 and 77 K.

Time-resolved emission decays were obtained following excitation by a PRA LN102 dye laser pumped by an LN100 N_2 laser. Lasing at 457 nm was achieved by coumarin 460 (Exciton). Emission was monitored at right angles to the excitation by using a Hamamatsu R3896 PMT coupled to a Macpherson 272 scanning monochromator. The output of the PMT was processed by a LeCroy 7200A transient digitizer interfaced to an IBM-PC. Transient decays were fit to single- and double-exponential functions by using the nonlinear least-squares Marquardt algorithm.

Transient absorption data were obtained following pulsed right-angle or collinear excitation at 460 nm (coumarin 460) or 420 nm (stilbene 420) by a Quanta-Ray PDL-2 dye laser pumped by the third harmonic of a Q-switched Quanta-Ray DCR-2A Nd-YAG laser (355 nm). The probe beam was produced by a 150 W Xe arc lamp operated in pulsed mode. The resulting beam was monitored by a five-stage R446 PMT coupled to an APL *f*/3.4 monochromator. The signal was processed by a LeCroy 7200A transient digitizer interfaced to an IBM-PC, and the data analyzed as for emission decay.

Temperature control of the solutions for emission studies was achieved by using a Janis NDT-6 cryostat with a Lakeshore DRC-84C temperature controller. The samples were allowed to equilibrate for 30 min at each temperature setting prior to data collection (except when measurements were taken at 2 K intervals, in which case 10 min was allowed for equilibration). To ensure that temperature equilibration had occurred, in random cases a second set of data at the same temperature was acquired after a further 10 min interval. In all cases examined, no significant differences between the two data sets were observed, indicating that the samples had equilibrated. An Oxford DN 1704 cryostat with an Oxford 3120 temperature controller was employed for transient absorption studies. In this case, the temperature at the sample was independently measured with an external thermocouple attached to the cell. During the course of the transient absorption measurements, the temperature was observed to shift by 10 K. Therefore, all temperatures are quoted as the average temperature (±5 K). Solutions were contained within cells of our own design for the low-temperature experiments and were freeze−pump−thaw degassed (3−4 cycles at $<10^{-5}$ Torr) before sealing.

Computer fitting of the steady-state emission spectra according to a Franck−Condon analysis was carried out as outlined previously.[19,20]

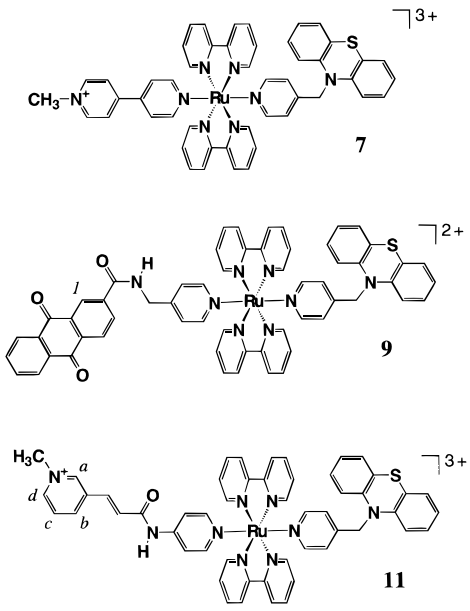

Figure 1. Structures of the chromophore−quencher triads *trans*-$[Ru(bpy)_2(py\text{-}PTZ)(MQ^+)]^{3+}$ (**7**), *trans*-$[Ru(bpy)_2(py\text{-}PTZ)(py\text{-}AQ)]^{2+}$ (**9**), and *trans*-$[Ru(bpy)_2(py\text{-}PTZ)(py\text{-}MPAA)]^{3+}$ (**11**).

Results

Synthesis. The *trans* geometry and structures of the ligands used in this study are illustrated in Figure 1. The symmetrical triad salts **3-PF$_6$** and **4-PF$_6$** were prepared directly from *trans*-$[Ru(bpy)_2(H_2O)_2](CF_3SO_3)_2$ by reaction with an excess of ligand in DMF at 100 °C. In both cases similarly high yields of complex are obtained, but recrystallization is required in order to obtain the bis-(py-PTZ) salt **4-PF$_6$** in pure form. Previous workers have prepared the salt *trans*-$[Ru(bpy)_2(py)_2](ClO_4)_2$ in 51% yield simply by heating *trans*-$[Ru(bpy)_2(H_2O)_2](ClO_4)_2$ in pyridine at reflux.[21]

The asymmetrical dyad and triad complexes were prepared by adaptations of a previously described synthetic methodology.[12] The salt **1-CF$_3$SO$_3$** was obtained from the reaction between *trans*-$[Ru(bpy)_2(H_2O)_2](CF_3SO_3)_2$ and an excess of py-PTZ in DMSO/acetone at room temperature. An extended reaction time was required, in comparison to the previously described synthesis of *trans*-$[Ru(bpy)_2(4\text{-}Etpy)(DMSO)](PF_6)_2$, because of the lower ligand concentration.[12] The chloro

(18) (a) Harrigan, R. W.; Crosby, G. A. *J. Chem. Phys.* **1973**, *59*, 3468. (b) Demas, J. N.; Crosby, G. A. *J. Phys. Chem.* **1971**, *75*, 991.

(19) (a) Claude, J. P. Ph.D. Dissertation, The University of North Carolina at Chapel Hill, 1995. (b) Claude, J. P.; Meyer, T. J. *J. Phys. Chem.* **1995**, *99*, 51.

(20) (a) Caspar, J. V.; Westmoreland, T. D.; Allen, G. H.; Bradley, P. G.; Meyer, T. J.; Woodruff, W. J. *J. Am. Chem. Soc.* **1984**, *106*, 3492. (b) Kober, E. M.; Caspar, J. V.; Lumpkin, R. S.; Meyer, T. J. *J. Phys. Chem.* **1986**, *90*, 3722.

(21) Walsh, J. L.; Durham, B. *Inorg. Chem.* **1982**, *21*, 329.

Table 1. Electrochemical Data for *trans*-$[Ru(bpy)_2(py^a)(py^b)]^{n+}$ in acetonitrile 0.1 M in $[N(C_4H_9\text{-}n)_4]PF_6$

				$E_{1/2}$, V vs SCE[a]					
compd. no.	py^a	py^b	n	$Ru^{III/II}$	$PTZ^{+/0}$	$MQ^{+/0}$	$AQ^{0/-}$	$MPAA^{0/-}$	$bpy^{0/-}$
3	MQ^+	MQ^+	4	1.35		−0.77			
4	py-PTZ	py-PTZ	2	1.32	0.83				−1.27
5	py-PTZ	4-Etpy	2	1.33	0.83				−1.27
6	MQ^+	4-Etpy	3	1.31		−0.79			−1.23
7	MQ^+	py-PTZ	3	1.32	0.83	−0.75			−1.27
8	4-Etpy	py-AQ	2	1.25			−0.77		
9	py-PTZ	py-AQ	2	*b*	0.88		−0.71		
10	4-Etpy	py-MPAA	3	1.22				−1.02[c]	−1.28
11	py-PTZ	py-MPAA	3	1.26	0.84			−1.03[c]	−1.28

[a] At a Pt-disk working electrode (surface area 0.031 cm^2) at a scan rate of 200 mV s^{-1} with a ferrocene internal reference: $E_{1/2} = 0.41-0.42$ V, $\Delta E_p = 85-100$ mV. [b] In DMF 0.1 M in $[N(C_4H_9\text{-}n)_4]PF_6$. The $Ru^{III/II}$ couple is obscured by the solvent background in DMF. Solutions were *ca.* 10^{-3} M in complex. [c] $E_{p,c}$, irreversible reduction.

derivative **2-CF_3SO_3** was obtained from **1-CF_3SO_3** in a manner similar to the preparation of *trans*-$[RuCl(bpy)_2(4\text{-Etpy})]PF_6$,[12] with a slightly lower yield after purification. Metathesis of **1-CF_3SO_3** to the less soluble salt *trans*-$[Ru(bpy)_2(py\text{-PTZ})(DMSO)](PF_6)_2$ prior to reaction with LiCl affords *trans*-$[Ru(bpy)_2(py\text{-PTZ})Cl]PF_6$ in yield identical with that for **2**.

The asymmetrical bis(pyridyl) complexes **5-PF_6**−**11-PF_6** were prepared by chloride abstraction from **2-CF_3SO_3** or from *trans*-$[Ru(bpy)_2(4\text{-Etpy})Cl](PF_6)$, by a procedure similar to that previously used to synthesize *trans*-$[Ru(bpy)_2(4\text{-Etpy})(ISNE)](PF_6)_2$ (ISNE = ethyl isonicotinate).[12] Extended reaction times were required, except when using 4-Etpy, owing to the low ligand concentrations. Yields were generally higher (≥90%), except in the cases of **7-PF_6**, **8-PF_6**, and **9-PF_6**. An important factor in these reactions is that the chloride substitution proceeds more rapidly as the concentration of water is increased. With a water-soluble ligand such as 4-Etpy this presents no problem, but it becomes a limiting factor when using the much less soluble ligand py-AQ, hence the low yields obtained for **8-PF_6** and **9-PF_6**. It should also be noted that the low solubility and photosensitive nature of the *trans*-bis(pyridyl) products renders the use of chromatographic purification unfeasible. This, along with the necessity for mild reaction conditions and other experimental nuances, can render the isolation of pure products a laborious and time-consuming process.

Electrochemistry and UV−Visible Absorption Spectra. Redox potentials measured by cyclic voltammetry are reported in Table 1. These values are similar to those found for other Ru(II) and Re(I) complexes containing identical or related ligands.[9,22,23] For py-MPAA, only an irreversible reduction is reported. This behavior has been noted before and may to be due to polymerization initiated by the MPAA radical.[16,22]

Absorption maxima in DMSO are reported in Table 2. Spectral assignments follow from those for *trans*-$[Ru(bpy)_2(4\text{-Etpy})_2]^{2+}$, $[Ru(bpy)(tpm)(R\text{-py})]^{2+}$ (tpm = tris(1-pyrazolyl)-methane), and $[Ru(tpm)(bpy)(MQ^+)]^{3+}$.[9,24] The near-UV (340−380 nm) and visible regions of the spectrum are dominated by $d\pi(Ru) \rightarrow \pi^*(bpy)$ MLCT bands. The intense UV bands at 262−265 and 292−300 nm arise from $\pi \rightarrow \pi^*$ transitions centered on the bpy ligand. For complexes containing MQ^+, the observed MLCT absorptions are a superposition of the Ru(II) → bpy and Ru(II) → MQ^+ bands, which appear at approximately the same energy.[9,25]

Table 2. Absorption (in DMSO at Room Temperature) and Emission (in 2-Methyltetrahydrofuran at 145 K) for *trans*-$[Ru(bpy)_2(py^a)(py^b)]^{n+}$

				absorption λ_{max}, nm[a] (ϵ, M^{-1} cm^{-1})		emission[b]
entry no.	py^a	py^b	n	$\pi \rightarrow \pi^*$	MLCT	λ_{max}, nm
1	py-PTZ	DMSO	2	262 (37 900) 292 (41 100)	416 (8 300)	
2	py-PTZ	Cl	1	264 (29 900) 304 (39 600)	374 (11 300) 518 (10 400) 542 (9 900)	
3	MQ+	MQ+	4	264 (51 100) 296 (47 600)	470 (26 500)	
4	py-PTZ	py-PTZ	2	264 (44 500) 300 (46 900)	350 (17 700) 486 (11 900)	
5	py-PTZ	4-Etpy	2	262 (36 300) 300 (46 200)	348 (17 300) 488 (12 600)	647
6	MQ+	4-Etpy	3	264 (36 400) 298 (47 700)	480 (18 400)	645, 820[c]
7	MQ+	py-PTZ	3	262 (49 900) 298 (46 500)	478 (18 700)	606
8	py-AQ	4-Etpy	2	264 (48 200) 300 (45 150)	340 (20 050) 488 (12 100)	651
9	py-AQ	py-PTZ	2	264 (63 700) 300 (49 200)	338 (22 600) 486 (12 600)	645
10	py-MPAA	4-Etpy	3	265 (30 750) 300 (58 750)	366 (15 250) 490 (12 000)	657
11	py-MPAA	py-PTZ	3	262 (48 500) 300 (61 750)	370 (17 050) 490 (12 100)	654

[a] Recorded in DMSO at concentrations *ca.* 10^{-5} M. [b] Recorded in deaerated 2-methyltetrahydrofuran at 145 K. [c] Maxima reflect both $Ru^{III}-bpy^{\bullet-}$ and $Ru^{III}-MQ^{\bullet}$ emission; see text.

Photophysics. The complexes *trans*-$[Ru(bpy)_2(py\text{-PTZ})_2]^{2+}$ (**4**) and *trans*-$[Ru(bpy)_2(py\text{-PTZ})(4\text{-Etpy})]^{2+}$ (**5**) are nonemissive at room temperature in CH_3CN and in 4/5 (v/v) propionitrile/butyronitrile. Irradiation at room temperature leads to photodecomposition, as evidenced by changes in the MLCT absorption spectra. Similar behavior has been noted for the model complex *trans*-$[Ru(bpy)_2(4\text{-Etpy})_2]^{2+}$, which in CH_3CN undergoes stepwise photosubstitution at room temperature upon MLCT irradiation with a quantum yield of 0.49 for the first step in eq 2.[26]

$$trans\text{-}[Ru(bpy)_2(4\text{-Etpy})_2]^{2+} + CH_3CN \xrightarrow{h\nu} cis\text{-}[Ru(bpy)_2(4\text{-Etpy})(CH_3CN)]^{2+} + 4\text{-Etpy} \quad (2)$$

At 77 K in a 4/5 (v/v) propionitrile/butyronitrile glass, these complexes show emission typical of Ru(II) polypyridyls: for **4**, $\lambda_{max} = 610$ nm, $\phi_{em} = 0.25$, and $\tau_{obs} = 3.40$ μs; for **5**, $\lambda_{max} = 610$ nm, $\phi_{em} = 0.26$, and $\tau_{obs} = 3.43$ μs; for *trans*-$[Ru(bpy)_2$-

(22) Katz, N. E.; Mecklenburg, S. L.; Meyer, T. J. *Inorg. Chem.* **1995**, *34*, 1282.
(23) Opperman, K. A.; Mecklenburg, S. L.; Meyer, T. J. *Inorg. Chem.* **1994**, *33*, 5295.
(24) Myrick, M. L.; Blakley, R. L.; De Armond, M. K. *J. Phys. Chem.* **1989**, *93*, 3936.
(25) Bates, W. D.; Chen, P.; Bignozzi, C. A.; Schoonover, J. R.; Meyer, T. J. *Inorg. Chem.* **1995**, *34*, 6215.
(26) Thompson, D. W.; Schoonover, J. R.; Graff, D.; Treadway, J.; Meyer, T. J. Manuscript in preparation.

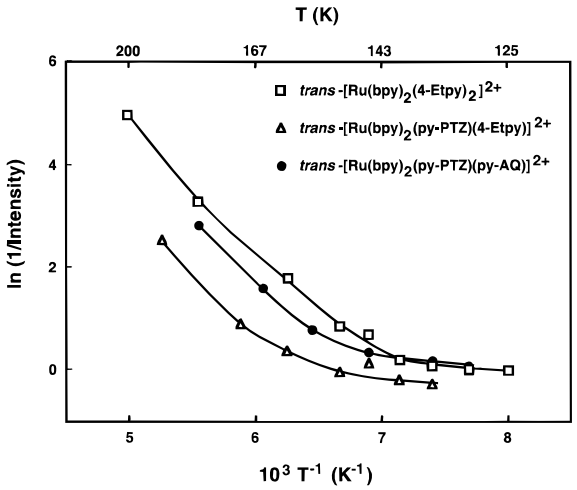

Figure 2. Emission intensities as a function of temperature for *trans*-$[Ru(bpy)_2(4\text{-}Etpy)_2]^{2+}$ and *trans*-$[Ru(bpy)_2(4\text{-}Etpy)(py\text{-}PTZ)]^{2+}$ (4:5 propionitrile/butyronitrile solvent) with 460 nm excitation and for *trans*-$[Ru(bpy)_2(py\text{-}PTZ)(py\text{-}AQ)]^{2+}$ (2-methyltetrahydrofuran solvent) with 480 nm excitation.

$(4\text{-}Etpy)_2]^{2+}$, $\lambda_{max} = 608$ nm, $\phi_{em} = 0.22$, and $\tau_{obs} = 3.40$ μs. In the emission spectral profile for **5** at 77 K a vibronic structure appears with a spacing of 1330 cm^{-1}, similar to those for other Ru(II) polypyridyl complexes.[27,28] The corresponding excitation profile displays a vibronic structure with 670 cm^{-1} progressions, which is typical for *trans*-$[Ru(bpy)_2(py)_2]^{2+}$ but is not observed for $[Ru(bpy)_3]^{2+}$ and other *cis*-$[Ru(bpy)_2L_2]^{2+}$ complexes.[24,26] The distinctive excitation spectrum is an excellent spectral tag for the detection of photodecomposition.

Emission maxima for **5** undergo a red shift from 616 nm in the rigid nitrile glass at 77 K to 650 nm in the fluid at 160 K. Such shifts are a characteristic feature of Ru(II) polypyridyl and other MLCT excited states.[27,29] The temperature dependence of relative emission quantum yields (ϕ_{em}^{rel}, relative to the emission intensity at 125 K) from 125 to 190 K for *trans*-$[Ru(bpy)_2(4\text{-}Etpy)_2]^{2+}$, **5**, and **9** are shown in Figure 2. The decrease at 145−150 K is accompanied by photodecomposition of *trans*-$[Ru(bpy)_2(4\text{-}Etpy)_2]^{2+}$, as shown by changes in the excitation and emission spectra with time. The temperature dependence of ϕ_{em}^{rel} for **5** is similar to that of the 4-Etpy model complex, and it was not possible to search for photoinduced electron transfer above 145 K due to its photoinstability.

The temperature dependence of the emission lifetime of **5** was determined in the range 115−150 K. The data are presented in Table 3. Single-exponential decays were observed from 115 to 130 K comparable in magnitude to those for *trans*-$[Ru(bpy)_2(4\text{-}Etpy)_2]^{2+}$: $\tau(130\text{ K}) = 1.6$ μs for **5** and 1.4 μs for *trans*-$[Ru(bpy)_2(4\text{-}Etpy)_2]^{2+}$. Decay kinetics above 130 K are nonexponential, and significant changes occurred in MLCT absorption spectra before and after the experiment, indicating appreciable photodecomposition. The appearance of nonexponential kinetics may be due to intrinsic factors, an emitting photogenerated impurity, or both.

Steady-state emission spectra for *trans*-$[Ru(bpy)_2(L)(py\text{-}AQ)]^{2+}$ (**8**, **9**) and *trans*-$[Ru(bpy)_2L(py\text{-}MPAA)]^{3+}$ (**10**, **11**), where L = 4-Etpy and py-PTZ, respectively, are similar at low temperature in 2-methyltetrahydrofuran. Emission maxima at 145 K occur at 651 nm (**8**), 645 nm (**9**), 657 nm (**10**), and 654 nm (**11**). Application of a Franck−Condon analysis[19,20] to the emission profile for **9** at 145 K reveals a 1300 cm^{-1} ν(bpy) progression with E_o occurring at 15 460 cm^{-1}. Similar analysis for **11** gave a 1310 cm^{-1} progression with E_o occurring at 15 310 cm^{-1} (Supplementary Table 1; Supporting Information). The temperature dependence of the emission intensity from **9** follows that for *trans*-$[Ru(bpy)_2(4\text{-}Etpy)_2]^{2+}$ and *trans*-$[Ru(bpy)_2(4\text{-}Etpy)(py\text{-}PTZ)]^{2+}$ (Figure 2), with the transition to a highly temperature-dependent regime occurring at 150 K. For **11**, the emission maximum shifts from 624 nm in a 2-methyltetrahydrofuran glass at 125 K to 655 nm in fluid solution at 155 K.

Time-resolved emission decay measurements reveal that all of these complexes exhibit primarily single-exponential decay in the range 125−205 K (Table 3). A small component with a lifetime <20 ns appeared at shorter wavelengths (610−615 nm). This feature was of varying magnitude for the different samples, and its origin is probably a small amount of an emitting impurity.

Data for the temperature dependence of the decay rate constant k_{obs} ($=\tau^{-1}$) for *trans*-$[Ru(bpy)_2(4\text{-}Etpy)(py\text{-}MPAA)]^{3+}$ (**10**) are listed in Table 3. Again, as for *trans*-$[Ru(bpy)_2(4\text{-}Etpy)_2]^{2+}$, a transition to a strongly temperature-dependent regime is observed near 150 K. These data could be satisfactorily fit to the expression in eq 3, which has been used to fit temperature-dependent decay data for related Ru(II) polypyridyl complexes.[20,28,30]

$$[\tau_0(T)]^{-1} = k_1 + k_2 \exp[-\Delta E_2/k_B T] \qquad (3)$$

For complex **10**, the following values are obtained from this analysis in the temperature range 140−190 K: $\Delta E_2 = 2470 \pm 30$ cm^{-1}, $k_2 = [1.1(\pm 0.2)] \times 10^{15}$ s^{-1}, and $k_1 = [9.6(\pm 0.2)] \times 10^5$ s^{-1} (Figure 3). The values for k_{obs} are included as Supporting Information; values below 140 K were not used due to contributions to the kinetics from the glass−fluid transition.[29,31] For comparison, the temperature-dependent emission intensities for *trans*-$[Ru(bpy)_2(4\text{-}Etpy)_2]^{2+}$ (Figure 2), when fitted to the same function, yield $\Delta E_2 = 2130 \pm 40$ cm^{-1}. In this treatment it is assumed that k_1, which is the sum of the nonradiative (k_{nr}) and radiative (k_r) rate constants for the emitting MLCT state(s), is relatively independent of temperature in the range studied.[19b]

The photochemical instability of these complexes precluded transient absorption measurements at room temperature. However, low-temperature transient absorption measurements were performed for the triads in 2-methyltetrahydrofuran in order to search for photoinduced electron-transfer intermediates. For *trans*-$[Ru(bpy)_2(py\text{-}PTZ)(py\text{-}AQ)]^{2+}$, no absorption features which could be attributed to the presence of anthraquinone radical anion ($\lambda_{max} = 590$ nm) or phenothiazine radical cation ($\lambda_{max} = 517$ nm) were observed at 140 K or at 190 K.[6c,23,32,33] Negative absorption at 510 nm and a positive feature at 390 nm (corresponding to a ground-state bleach and formation of a

(27) Meyer, T. J. *Pure Appl. Chem.* **1986**, *58*, 1193.
(28) (a) Rillema, D. P.; Blanton, C. B.; Shaver, R. J.; Jackman, D. C.; Boldaji, M.; Bundy, S.; Worl, L. A.; Meyer, T. J. *Inorg. Chem.* **1992**, *31*, 1600. (b) Barqawi, K. R.; Llobet, A.; Meyer, T. J. *J. Am. Chem. Soc.* **1988**, *110*, 7751. (c) Allen, G. H.; White, R. P.; Rillema, D. P.; Meyer, T. J. *J. Am. Chem. Soc.* **1984**, *106*, 2613. (d) Caspar, J. V.; Meyer, T. J. *Inorg. Chem.* **1983**, *22*, 2444. (e) Caspar, J. V.; Meyer, T. J. *J. Am. Chem. Soc.* **1983**, *105*, 5583.
(29) (a) Juris, A.; Balzani, V.; Barigelletti, F.; Campagna, S.; Belser, P.; von Zelewsky, A. *Coord. Chem. Rev.* **1988**, *84*, 85. (b) Barigelletti, F.; Belser, P.; von Zelewsky, A.; Juris, A.; Balzani, V. *J. Phys. Chem.* **1985**, *89*, 3680.
(30) Maruszewski, K.; Strommen, D. P.; Kincaid, J. R. *J. Am. Chem. Soc.* **1993**, *115*, 8345.
(31) (a) Danielson, E.; Lumpkin, R. S.; Meyer, T. J. *J. Phys. Chem.* **1987**, *91*, 1305. (b) Lumpkin, R. S.; Meyer, T. J. *J. Phys. Chem.* **1986**, *90*, 5307.
(32) Alkaitis, S. A.; Beck, G.; Grätzel, M. *J. Am. Chem. Soc.* **1975**, *97*, 5723.
(33) Nakayama, T.; Ushida, K.; Hamanoue, K.; Washio, M.; Tagawa, S.; Tabata, Y. *J. Chem. Soc., Faraday Trans.* **1990**, *86*, 95.

Table 3. Temperature Dependence of Emission Decay Constants ($k_{obs} = \tau^{-1}$) for *trans*-$[Ru(bpy)_2(py^a)(py^b)]^{n+}$

	$10^{-5}k_{obs}$ (s^{-1})				
temp (K)	py^a = py-PTZ, py^n = 4-Etpy[a]	py^a = 4-Etpy, py^n = py-AQ[c]	py^a = py-PTZ, py^n = py-AQ[c]	py^a = 4-Etpy, py^b = py-MPAA[c]	py^a = py-PTZ, py^b = py-MPAA[c]
115	4.06				
120	4.90			5.78	
125	5.61	6.99	5.96	7.21	5.47
130	6.21			7.60	
135		7.70	6.81	8.49	7.20
140	6.66[b]			8.95	
145		8.73	8.32	9.91	9.28
150	7.61[b]			10.3	
155		12.1	13.1	11.2	11.2
160				12.3	
165		24.9	29.1	14.4	16.3
170				18.7	
175		64.9	81.2	25.2	30.7
180				37.3	
185				60.4	73.6
190		300	320	89.2	
195				150	170

[a] Conditions: in deaerated 4/5 (v/v) propionitrile/butyronitrile; excitation wavelength 457 nm; monitoring emission wavelength 620 nm. [b] Some double-exponentiality observed above 140 K. The value reported is for the best single-exponential fit. [c] Conditions: in deaerated 2-methyltetrahydrofuran; excitation wavelength 457 nm; monitoring wavelength 650 nm.

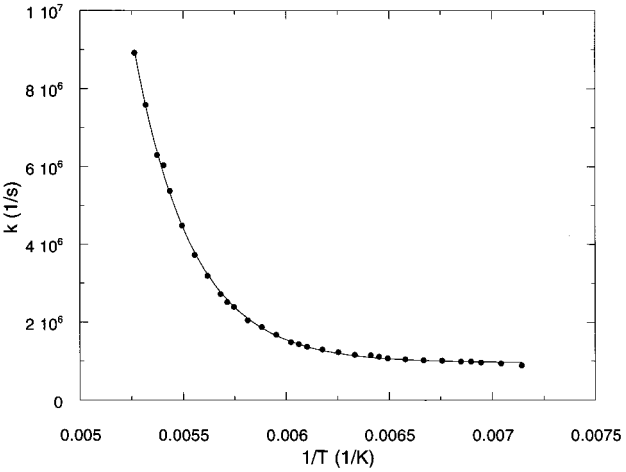

Figure 3. Temperature dependence of the emission decay rate constant k_{obs} for *trans*-$[Ru(bpy)_2(4\text{-Etpy})(py\text{-MPAA})]^{3+}$, with calculated fit from eq 3. Fitting parameters: $\Delta E_2 = 2470 \pm 30$ cm^{-1}, $k_2 = [1.1(\pm 0.2)] \times 10^{15}$ s^{-1}, and $k_1 = [9.6(\pm 0.2)] \times 10^5$ s^{-1}.

bipyridine radical anion) were observed. These features are consistent with an MLCT excited state. They decay exponentially with $k_{obs} = [6.4(\pm 1.2)] \times 10^5$ s^{-1} at 140 K, parallel to emission decay.

The decay of the transient absorption spectrum of *trans*-$[Ru(bpy)_2(py\text{-PTZ})(py\text{-MPAA})]^{3+}$ with time is illustrated in Figure 4a. Again, the main feature is the ground-state bleach, which decays exponentially with $k = 9.0 \times 10^5$ s^{-1} at 140 K. There is evidence for additional features. A small absorption at 520−550 nm ($k_{obs} = 7.3 \times 10^5$ s^{-1}) suggests the presence of $-PTZ^{\bullet+}$, and an extremely small feature at 430−440 nm superimposed on the ground-state bleach is consistent with formation of a small concentration of pyridinium radical on the py-MPAA ligand due to oxidative quenching of the $Ru^{III}-bpy^{\bullet-}$ MLCT state.[22] At 180 K, the rate of decay of the 540 nm feature is increased: $k_{obs} = 5.3 \times 10^6$ s^{-1}. At higher temperatures, photochemical decomposition is accelerated. Room-temperature acetonitrile solutions of *trans*-$[Ru(bpy)_2(py\text{-PTZ})(py\text{-MPAA})]^{3+}$, although relatively stable thermally, undergo rapid changes in MLCT absorption spectra with 480 nm irradiation from a 150 W Xe lamp after a 15 s irradiation period.[34]

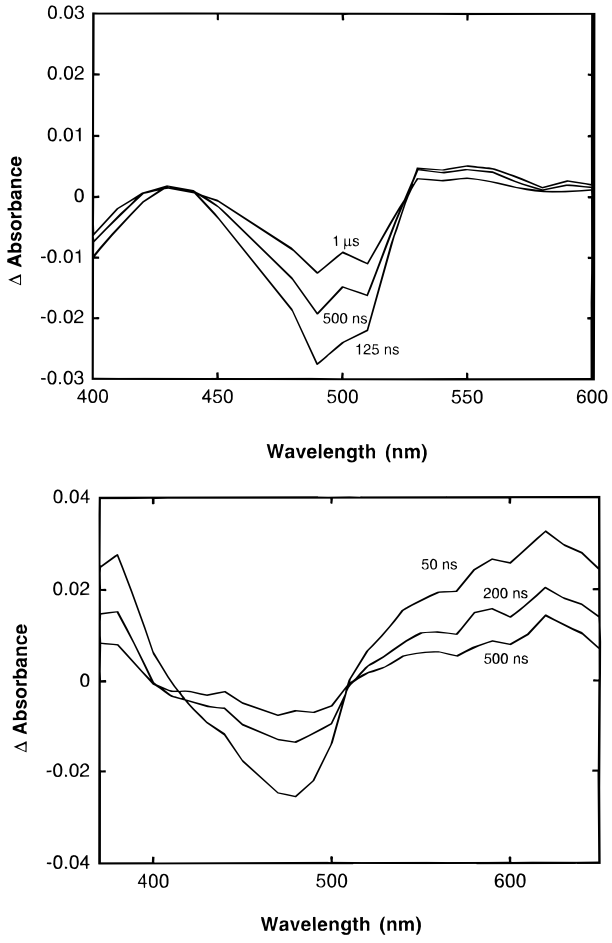

Figure 4. Transient absorption difference spectra at 140 K in 2-methyltetrahydrofuran for (a, top) *trans*-$[Ru(bpy)_2(py\text{-PTZ})(py\text{-MPAA})](BAr_4)_3$ and (b, bottom) *trans*-$[Ru(bpy)_2(py\text{-PTZ})(MQ^+)](BAr_4)_3$ upon excitation at 460 nm.

Low-temperature emission spectra for *trans*-$[Ru(bpy)_2(MQ^+)_2]^{4+}$ (**3**), *trans*-$[Ru(bpy)_2(4\text{-Etpy})(MQ^+)]^{3+}$ (**6**), and *trans*-$[Ru(bpy)_2(py\text{-PTZ})(MQ^+)]^{3+}$ (**7**) are typical of MLCT emitters. At 77 K in 4/5 propionitrile/butyronitrile, λ_{max} and ϕ_{em} were

(34) Adelt, M.; Devenney, M.; Friesen, D. A. Unpublished results.

590 nm and 0.26 for **3** and 598 nm and 0.27 for **6**. Emission decay lifetimes were 4.3 μs ($k_{obs} = 2.33 \times 10^5$ s^{-1}) (**3**) and 3.7 μs ($k_{obs} = 2.70 \times 10^5$ s^{-1}) (**6**). A slight degree of nonexponentiality was observed, analogous to observations made earlier for [Ru(tpm)(bpy)(MQ$^+$)]$^{3+}$.[9] This arises because these complexes possess two emitting, kinetically coupled MLCT states, Ru^{III}(bpy$^{\bullet-}$) and Ru^{III}(MQ$^{\bullet}$).

The degree of nonexponential character for *trans*-[Ru(bpy)$_2$(py-PTZ)(MQ$^+$)]$^{3+}$ is greatly enhanced at higher temperatures in the fluid (see below). At 77 K in the same glassy medium, emission decay at the maximum of 599 nm is exponential with $\tau = 3.51$ μs ($k_{obs} = 2.85 \times 10^5$ s^{-1}).

Emission for these complexes is markedly temperature dependent, as illustrated by the steady-state emission spectrum of *trans*-[Ru(bpy)$_2$(4-Etpy)(MQ$^+$)]$^{3+}$ (**6**) in 2-methyltetrahydrofuran in Figure 5a. At 130 K, two maxima are observed, at 636 and 817 nm. The intensity of the latter is increased relative to that of the former at higher temperatures, and by 145 K it represents the dominant emission. The broad nature of this band is consistent with emission from the Ru^{III}(MQ$^{\bullet}$) MLCT state.[9,35] Very similar behavior has been observed for *cis*-[Ru(bpy)$_2$(MQ$^+$)$_2$]$^{4+}$.[36] The Ru^{III}(MQ$^{\bullet}$) state is presumably the dominant state under these conditions. In order MQ$^+$ complexes ϕ_{em} is relatively small.[9,37] The presence of an analogous low-energy emission in low-temperature spectra of *trans*-[Ru(bpy)$_2$(py-PTZ)(MQ$^+$)]$^{3+}$ (**7**) is not obvious. However, an increase in intensity to the red side of the emission maximum at 586−606 nm with increasing temperature (Figure 5b) suggests that such an emission may be present.

Emission decay from **6** and **7** in 4/5 (v/v) propionitrile/butyronitrile is nonexponential but could be fit to the double-exponential function in eq 4.

$$I(t) = A \exp(-k_1 t) + (1 - A) \exp(-k_2 t) \qquad (4)$$

In this equation, $I(t)$ represents the emission intensity as a function of time, k_1 and k_2 are the fitted decay constants for the two components, and A and $1 - A$ are the fitted amplitudes at time zero. The data are listed in Table 4.

Although the temperature and monitoring wavelength dependences are complex, several trends are apparent. For both complexes, k_1 and k_2 increase with increasing temperature. For *trans*-[Ru(bpy)$_2$(4-Etpy)(MQ$^+$)]$^{3+}$ at 130 K, both k_1 and k_2 increase as the monitoring wavelength increases from 630 nm (mainly Ru^{III}−bpy$^{\bullet-}$) to 800 nm (mainly Ru^{III}−MQ$^{\bullet}$). The contribution from the k_2 component also increases with monitoring wavelength. Absorption spectra in the MLCT region before and after the temperature-dependent lifetime studies on **6** and **7** show that minimal photodecomposition had occurred, demonstrating that both are more photostable than *trans*-[Ru(bpy)$_2$(4-Etpy)(py-PTZ)]$^{2+}$ (**5**) or *trans*-[Ru(bpy)$_2$(4-Etpy)$_2$]$^{2+}$.

There is evidence for the formation of *trans*-[Ru^{III}(bpy)$_2$(4-Etpy)(MQ$^{\bullet}$)]$^{3+}$ * following laser flash photolysis of **6** at 180 K. The prompt formation of a transient positive absorption feature at 610 nm is observed, but under these conditions the complex is photochemically unstable, as evidenced by visible spectra taken before and after the experiment. For *trans*-[Ru(bpy)$_2$(MQ$^+$)$_2$]$^{4+}$, spectra taken before and after the laser flash photolysis experiments reveal minimal decomposition. For **3**, positive absorption features at 370 and 610 nm ($\pi \rightarrow \pi^*$, MQ$^{\bullet}$) appear immediately upon laser excitation at 420 nm.[3d,9,25,35,37] There is a prompt bleach at 460 nm, which is consistent with the loss of ground-state absorption subsequent to laser flash excitation. Wave forms at all wavelengths examined decay exponentially with $k_{obs} = [4.24(\pm 0.05)] \times 10^6$ s^{-1} ($\tau = 235$ ns).

The time-dependent decay of the transient absorption spectrum of *trans*-[Ru(bpy)$_2$(py-PTZ)(MQ$^+$)]$^{3+}$ in 2-methyltetrahydrofuran at 140 K is illustrated in Figure 4b. An intense absorption feature due to the MQ$^{\bullet}$ radical is observed at

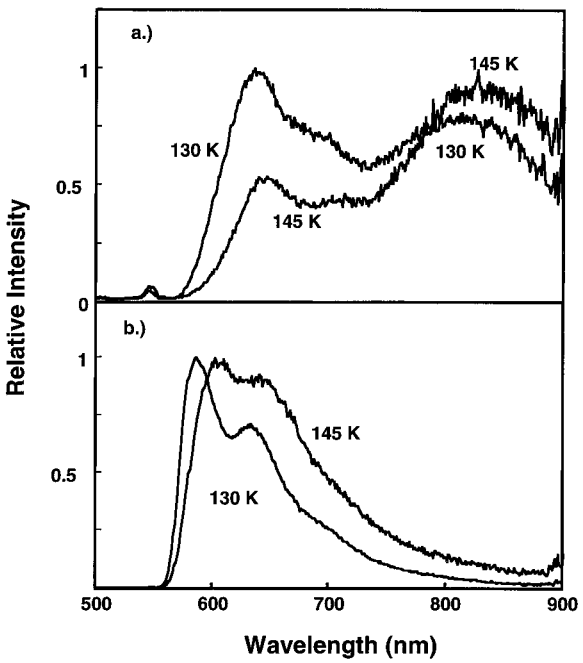

Figure 5. Steady-state emission spectra for (a, top) *trans*-[Ru(bpy)$_2$(4-Etpy)(MQ$^+$)](BAr$_4$)$_3$ and (b, bottom) *trans*-[Ru(bpy)$_2$(py-PTZ)(MQ$^+$)](BAr$_4$)$_3$ in 2-methyltetrahydrofuran. Excitation wavelength: 470 nm.

Table 4. Temperature and Monitoring Wavelength Dependence of Double-Exponential Emission Decays for *trans*-[Ru(bpy)$_2$(py^a)(py^b)]$^{3+}$ in Deaerated 4/5 (v/v) Propionitrile/Butyronitrile[a]

temp (K)	λ_{em} (nm)[b]	A	$10^{-5}k_1$ (s^{-1})	$10^{-6}k_2$ (s^{-1})
	A.*trans*-[Ru(bpy)$_2$(4-Etpy)(MQ$^+$)]$^{3+}$			
120	620	0.44	5.45	4.07
	660	0.44	5.01	3.99
	700	0.47	5.53	3.75
	750	0.43	6.12	3.61
130	630	0.41	4.56	7.35
	650	0.39	4.61	7.34
	700	0.39	4.61	7.34
	750	0.31	5.96	9.50
	800	0.25	10.5	9.23
145	630	0.44	5.52	57
	750	0.37	7.28	47
180	744	0.80	12.1	31
	B.*trans*-[Ru(bpy)$_2$(py-PTZ)(MQ$^+$)]$^{3+}$			
120	630	0.56	7.08	4.81
	660	0.51	6.99	5.48
	700	0.52	7.49	5.53
	750	0.40	8.68	6.82
130	630	0.35	6.90	10.1
	675	0.37	7.04	10.4
	720	0.33	8.12	12.3
145	630	0.44	10.4	31
180	700	0.36	18.5	46

[a] Excitation wavelength: 457 nm. Decay traces were fitted to eq 4. [b] Monitoring wavelength.

(35) Jones, W. E., Jr.; Chen, P.; Meyer, T. J. *J. Am. Chem. Soc.* **1992**, *114*, 387.
(36) Chen, P. Unpublished results.
(37) (a) Chen, P.; Danielson, E.; Meyer, T. J. *J. Phys. Chem.* **1988**, *92*, 3708. (b) Chen, P.; Meyer, T. J. Submitted for publication.

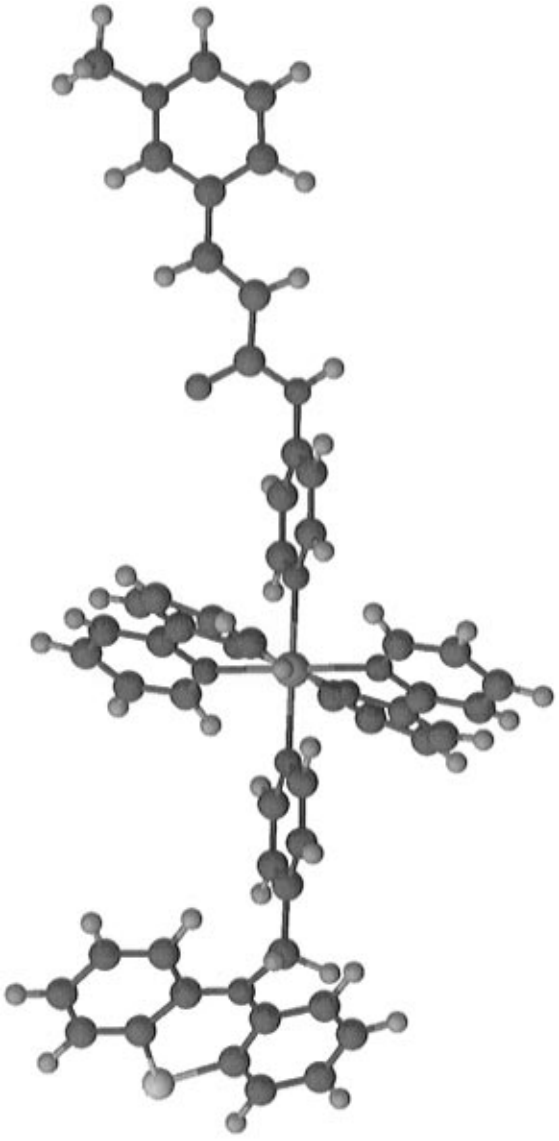

Figure 6. Structure of *trans*-[Ru(bpy)$_2$(py-PTZ)(py-MPAA)]$^{3+}$, obtained by using CAChe software.

approximately 600 nm. Absorption below 400 nm is a convolution of both MQ$^{\bullet}$ and bpy$^{\bullet-}$ $\pi-\pi^*$ bands. A prominent ground-state bleach is observed between 400 and 500 nm. These data were also fitted to a double-exponential decay function. At 140 K, the absorption at 370 nm and the bleach at 490 nm decay with the major component ($A = 0.78$) having $k_1 = [5.9(\pm0.7)] \times 10^6$ s^{-1} and $k_2 = [6.7(\pm0.1)] \times 10^5$ s^{-1}, A being the fraction of the total absorption change associated with the first component. At the same temperature, the MQ$^{\bullet}$ absorption at 600 nm decays with $k_1 = 7.0 \times 10^6$ s^{-1} ($A = 0.68$) and $k_2 = 8.5 \times 10^5$ s^{-1}. The fast component becomes more dominant as the temperature is increased. At 165 K, the absorption at 610 nm decays with $k_1 = 1.8 \times 10^7$ s^{-1} ($A = 0.87$) and $k_2 = 1.1 \times 10^6$ s^{-1}. At 175 K, the absorption at 385 nm decays with $k_1 = 3.4 \times 10^7$ s^{-1} ($A = 0.89$) and $k_2 = 2.5 \times 10^6$ s^{-1}. Absorption spectra taken before and after the experiment showed that photodecomposition had not occurred to any significant degree.

Discussion

The development of the stepwise synthetic methodology for the preparation of *trans*-[Ru(bpy)$_2$(py^a)(py^b)]$^{n+}$ complexes accomplishes a major goal. It allows for the placement of quencher substituents in the *trans* configuration around a bis(bipyridine)ruthenium(II) core, maximizing their spatial separation. This point is illustrated for the chromophore−quencher triad *trans*-[Ru(bpy)$_2$(py-PTZ)(py-MPAA)]$^{3+}$ in Figure 6. This figure was constructed by using the molecular mechanics optimization feature in CAChe software with an augmented MM2 force field. The crystal structure coordinates for the related *trans*-[Ru(Me$_2$bpy)$_2$(py)$_2$]$^{2+}$ ion were used for the geometry of the [Ru(bpy)$_2$] core.[38] In the figure, the distance between the centers of the pyridinium and phenothiazine substituents is ∼20 Å. An important feature from the electronic point of view is the methylene spacer to PTZ, which interrupts the extended π network. For comparison, the approximate distance between the -MQ$^+$ and -PTZ groups in [Ru(tpm)(bpy-PTZ)(MQ$^+$)]$^{3+}$ is 6 Å.[9]

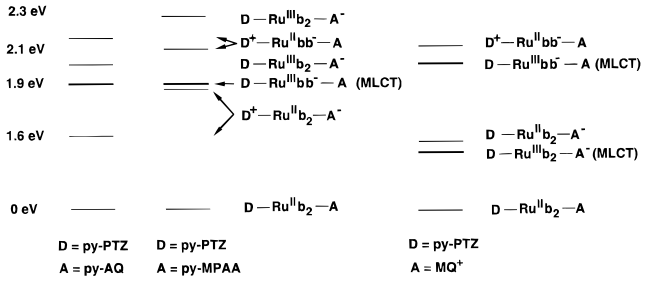

Figure 7. Approximate energy level diagrams for *trans*-[Ru(bpy)$_2$(py-PTZ)(py-AQ)]$^{2+}$, *trans*-[Ru(bpy)$_2$(py-PTZ)(py-MPAA)]$^{3+}$, and *trans*-[Ru(bpy)$_2$(py-PTZ)(MQ$^+$)]$^{3+}$.

Unfortunately, the goal of achieving long-lived redox separation in these complexes at room temperature was not realized due to photochemical instability. As in other polypyridyl complexes of Ru(II) containing bound pyridines, the complexes are highly unstable with regard to photochemical ligand loss. The mechanism is by thermal activation to and ligand loss from low-lying dd states.[39−41]

At lower temperatures (<150 K) where some degree of stability is attained, the production of -PTZ$^{\bullet+}$ and -A$^{\bullet-}$ in the triads (A = MQ$^+$, py-AQ, and py-MPAA) does not occur or is, at best, inefficient. The temperature-dependent photophysical properties of these complexes, *trans*-[Ru(bpy)$_2$(py^a)(py^b)]$^{n+}$ (py^a = 4-Etpy or py-PTZ, py^b = py-AQ or py-MPAA, $n = 2$ or 3), in terms of emission lifetimes and intensities are similar to those of other *cis*- and *trans*-(polypyridyl)ruthenium(II) complexes such as *trans*-[Ru(bpy)$_2$(4-Etpy)$_2$]$^{2+}$, which do not possess quencher ligands.[28] In these complexes, crossing to a low-lying dd state or states occurs at low temperatures and is accompanied by ligand loss.

The low-temperature onset of MLCT → dd conversion occurs before intramolecular electron transfer can occur to a significant degree. This is not surprising, given the energetics of electron transfer in the three chromophore−quencher assemblies. Approximate energy orderings are shown in Figure 7. These are only approximate, since they are derived from room-temperature redox potential measurements in CH_3CN or DMF (0.1 M in [(n-C_4H_9)$_4$N]PF_6) and E_o values calculated from emission spectra in 2-methyltetrahydrofuran at 145 K.

(38) Cordes, A. W.; Durham, B.; Swepston, P. N.; Pennington, W. T.; Condren, S. M.; Jensen, R.; Walsh, J. L. *J. Coord. Chem.* **1982**, *11*, 251.
(39) Henderson, L. J.; Cherry, W. R. *Chem. Phys. Lett.* **1985**, *114*, 553.
(40) (a) Durham, B.; Walsh, J. L.; Carter, C. L.; Meyer, T. J. *Inorg. Chem.* **1980**, *19*, 860. (b) Durham, B.; Caspar, J. V.; Nagle, J. K.; Meyer, T. J. *J. Am. Chem. Soc.* **1982**, *104*, 4803.
(41) (a) Pinnick, D. V.; Durham, B. *Inorg. Chem.* **1984**, *23*, 1440. (b) Pinnick, D. V.; Durham, B. *Inorg. Chem.* **1984**, *23*, 3842.

On the basis of the estimated energy levels in Figure 7, we make the following observations. (1) The redox-separated states *trans*-[Ru(bpy)$_2$(py-PTZ$^{\bullet+}$)(py-MPAA$^{\bullet-}$)]$^{3+}$ and *trans*-[Ru(bpy)$_2$(py-PTZ$^{\bullet+}$)(py-AQ$^{\bullet-}$)]$^{2+}$ are lowest lying or nearly lowest lying for *trans*-[Ru(bpy)$_2$(py-PTZ)(py-MPAA)]$^{3+}$ and *trans*-[Ru(bpy)$_2$(py-PTZ)(py-AQ)]$^{2+}$. (2) In either case, initial oxidative quenching to give D$-$Ru^{III}b$_2-$A$^{\bullet-}$ or reductive quenching to give D$^{\bullet+}-$Ru^{III}bb$^{\bullet-}-$A is thermodynamically uphill, creating a thermal barrier to the ultimate redox-separated state, D$^{\bullet+}-$Rub$_2-$A$^{\bullet-}$. (3) For *trans*-[Ru(bpy)$_2$(py-PTZ)(MQ$^+$)]$^{3+}$, initial oxidative quenching to give *trans*-[Ru(bpy)$_2$(py-PTZ$^{\bullet+}$)(MQ$^{\bullet}$)]$^{3+}$ is spontaneous and there is evidence that it occurs from the temperature-dependent transient measurements. However, in this case, and as found earlier for [Ru(tpm)(bpy-PTZ)(MQ$^+$)]$^{3+}$, this state lies *lower* than the redox-separated state. (4) For *trans*-[Ru(bpy)$_2$(py-PTZ)(py-MPAA)]$^{3+}$, there is evidence in the transient absorption difference spectrum for the redox-separated state, but MLCT $\rightarrow$ dd interconversion is overly competitive.

The conclusions are different for the three triads, but the effect is the same. The redox-separated state is not accessible to a significant degree because (1) it is not lowest-lying or (2) initial electron transfer is inhibited at low temperature by a thermal barrier. In any case, competitive MLCT $\rightarrow$ dd conversion and decomposition occur at temperatures above $\sim$150 K.

An additional nuance exists for the MQ$^+$-containing complexes *trans*-[Ru(bpy)$_2$(4-Etpy)(MQ$^+$)]$^{3+}$ and *trans*-[Ru(bpy)$_2$(py-PTZ)(MQ$^+$)]$^{3+}$. With MQ$^+$ as the acceptor ligand, the resulting Ru$^{III}-$MQ$^-$ MLCT state lies approximately 0.5 eV lower in energy than the Ru$^{III}-$bpy$^{\bullet-}$ state. This is shown by the 800$-$850 nm emission for *trans*-[Ru(bpy)$_2$(4-Etpy)(MQ$^+$)]$^{3+}$, in analogy to [Ru(tpm)(bpy)(MQ$^+$)]$^{3+}$.[9] The relative emission efficiencies are much lower ($\sim$4 times less for [Ru(tpm)(bpy)(MQ$^+$)]$^{3+}$ relative to [Ru(tpm)(bpy)(4-Etpy)]$^{2+}$ at room temperature) for the Ru$^{III}-$MQ$^{\bullet}$ excited states. In the rigid-glass matrix at 77 K, emission is overwhelmingly Ru$^{III}-$bpy$^{\bullet-}$-based; a similar effect has been noted for [Re(bpy)(CO)$_3$(MQ$^+$)]$^{2+}$. It is due to a rigid-medium effect arising from the frozen solvent dipoles in the rigid matrix.[37] Figure 5 shows that as the temperature is increased, the intensity of emission from the MQ$^{\bullet}$-based MLCT state increases relative to that from the bpy$^{\bullet-}$-based state. The presence of a substantial degree of nonexponentiality, even at 800 nm (where emission is mainly MQ$^{\bullet}$-based), for *trans*-[Ru(bpy)$_2$(4-Etpy)(MQ$^+$)]$^{3+}$ at 130 K indicates that decay of the two states is kinetically coupled to bpy$^{\bullet-}$ $\rightarrow$ MQ$^+$ electron transfer and occurs with $k \approx 10^5-10^6$ s^{-1}. This is illustrated in Scheme 1, which provides a summary of the MLCT photochemistry of *trans*-[Ru(bpy)$_2$(4-Etpy)(MQ$^+$)]$^{3+}$.

Scheme 1

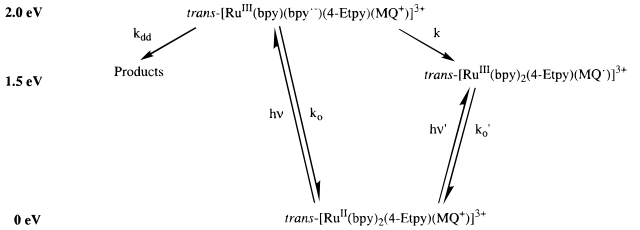

The rapid photodecomposition of *trans*-[Ru(bpy)$_2$(py-PTZ)(MQ$^+$)]$^{3+}$ upon room-temperature MLCT irradiation indicates that crossing to the photochemically reactive dd state (k_{dd} in Scheme 1) predominates at higher temperatures. Photodecomposition of *trans*-[Ru(bpy)$_2$(4-Etpy)(MQ$^+$)]$^{3+}$ is significant even at 180 K.

Acknowledgment. Support by the U.K. Science and Engineering Research Council under the NATO Postdoctoral Fellowship scheme (B.J.C.), the Natural Sciences and Engineering Research Council of Canada (D.A.F. and D.W.T.), and the National Science Foundation (Grant CHE-8806664) is gratefully acknowledged. We thank Kimberly A. Opperman for an initial sample of the py-AQ ligand prepared by an alternate route and Darryl S. Williams for a sample of the Na(BAr$_4$) salt.

Supporting Information Available: Tables describing the spectral fitting parameters for *trans*-[Ru(bpy)$_2$(py-PTZ)(py-MPAA)]$^{3+}$, *trans*-[Ru(bpy)$_2$(py-PTZ)(py-AQ)]$^{2+}$, and *trans*-[Ru(bpy)$_2$(py-PTZ)(4-Etpy)]$^{2+}$ and emission lifetimes for *trans*-[Ru(bpy)$_2$(4-Etpy)(py-MPAA)]$^{3+}$ used for the temperature-dependent fit (Figure 3) (2 pages). Ordering information is given on any current masthead page.

IC9515463